Ferrite Control in Duplex Stainless Steel Weld Metal

Although it has little influence on yield and tensile strength, controlling the EFN of the weld deposit has a marked effect on ductility

BY D. J. KOTECKI

Introduction

Duplex stainless steels in wrought or cast form, when they reach the user, consist of a microstructure of approximately 50% austenite and 50% ferrite. This mix of phases imparts very desirable properties to the material over a useful service temperature range from as low as −50°F (−46°C) to as high as 500°F (260°C), notably: yield strength nearly double that of wrought austenitic stainless steel, ductility and toughness approaching that of wrought austenitic stainless steel, and resistance to chloride stress corrosion cracking approaching that of wrought ferritic stainless steel. Table 1 lists composition and mechanical property limits for two duplex stainless steels of interest herein, as well as for Type 316 stainless steel, all in plate form, as specified by ASTM A240-85. The desirable microstructure of wrought or cast duplex stainless steel is obtained by heat treatment and/or hot working a structure that is initially much higher in ferrite content. The thermal treatment, generally in the temperature range of 1900° to 2100°F (1038° to 1149°C), causes part of the original ferrite to tranform to austenite by a diffusion controlled reaction.

A matching weld deposit, however, without the benefit of heat treatment or hot working, reverts back to a very high ferrite content. Autogenous welds or welds with matching filler metals in alloys like 22 Cr-5 Ni-3 Mo (hereinafter referred to as Alloy 2205) or 25 Cr-5 Ni-3 Mo-2 Cu (hereinafter referred to as Alloy 255) tend to be very brittle without an annealing heat treatment. Blumfield, Clark and Guha (Ref. 1) found it advisable to increase the nickel in weld filler metals for Alloy 255 in order to obtain even 10% elongation as-welded. Likewise, Bryhan and Poznansky (Ref. 2) employed a filler metal containing 9% nickel in an otherwise matching composition to successfully join Alloy 2205.

In the same work, Bryhan and Poznansky also examined corrosion behavior, including stress corrosion cracking, for the higher nickel weld metal, and found that the corrosion resistance of the weldment was only slightly reduced compared to the base metal. These researchers made no mention of the ferrite content of their weld metals. Blumfield, Clark and Guha, cited earlier, claimed that they obtained 80% austenite (determined by metallographic means) in Alloy 255 weld metal of 6.9% nickel, and found corrosion characteristics similar to those of the parent metal. In both the work of Blumfield, Clark and Guha and that of Bryhan and Poznansky, weld metal ductility in the enriched nickel weldments was below 20%, a value generally considered necessary to pass a 2T side bend test (a ⅜-in.-thick slice of weldment bent 180 deg around a ¾-in. radius). This criterion appears to have been ignored despite the fact that it is generally a part of a fabricator's procedure qualification.

Ferrite Determination

Metallographic determination of weld metal ferrite content in largely austenitic weld metal is a very uncertain undertaking because of the fineness and irregularity of the ferrite phase. In view of this, the Welding Research Council Advisory Subcommittee on Welding Stainless Steel (Ref. 3) rejected percent ferrite determinations as unreliable, and instead adopted a ferrite number system based upon magnetic attraction of a standard magnet to the weld metal.

This ferrite number system, as defined in Ref. 3, is not directly suitable for ferrite determinations in duplex stainless weld metals because the calibration range ends at 28 FN. Pleva and Nordin (Ref. 4) characterized duplex stainless weld metal ferrite contents using a "magnetic balance," but the calibration of this system is unknown to the writer. On the other hand, the writer has shown that the familiar ferrite number system, which is

Table 1—Composition and Mechanical Property Limits for Stainless Steel Plates

Type	316	2205	255
UNS Designation	S31600	S31803	S32550
C	0.08 max.	0.030 max.	0.04 max.
Mn	2.00 max.	2.00 max.	1.5 max.
P	0.045 max.	0.030 max.	0.040 max.
S	0.030 max.	0.020 max.	0.030 max.
Si	1.00 max.	1.00 max.	1.0 max.
Cr	16.00–18.00	21.0–23.0	24.0–27.0
Ni	10.00–14.00	4.50–6.50	4.5–6.5
Mo	2.00–3.00	2.50–3.50	2.0–4.0
Cu	–	–	1.5–2.5
N	0.10 max.	0.08–0.20	0.10–0.25
Tensile (ksi)	75 min.	90 min.	110 min.
Yield (ksi)	30 min.	65 min.	80 min.
% Elongation	40 min.	25 min.	15 min.

Paper presented at the 66th Annual AWS Meeting, held April 28 to May 3, 1985, in Las Vegas, Nev.

D. J. KOTECKI is Director of Research, Welding Products Division, Teledyne McKay, York, Pa.

Table 2—Alloy 2205 (22Cr-5Ni-3Mo) Experimental Welds

3/32-in. Flux Cored Open-Arc Electrodes

Expmt. no.	817	844	853	854	863	864
C	0.039	0.021	0.030	0.030	0.032	0.028
Mn	1.29	1.63	1.80	1.70	1.95	1.98
P	0.009	0.007	0.010	0.007	0.010	0.008
S	0.012	0.015	0.012	0.013	0.015	0.015
Si	0.26	0.26	0.30	0.28	0.32	0.32
Cr	21.02	20.99	20.80	20.33	22.23	22.24
Ni	5.37	6.75	7.45	7.90	7.96	8.40
Mo	3.00	3.09	2.92	2.80	3.40	3.37
Ti	0.15	0.13	0.13	0.13	0.13	0.08
N	0.154	0.095	0.093	0.093	0.118	0.114
EFN	75	76	62	40	61	49
Fe	68.7	67.0	66.5	66.7	63.8	63.4
EFN/NFN	1.517	1.485	1.474	1.479	1.424	1.417
NFN	49	51	42	27	43	35
UTS (ksi)	111.9	104.2	110.6	109.8	113.1	111.9
YS (ksi)	90.2	86.9	87.1	85.3	91.3	88.8
% Elongation	16.6	13	30.5	32	29	25
CVN@ −50°F (ft-lb)	7.3	17.4	30.1	35.9	24.3	24.3
mils	0.7	5.7	14.3	19.7	10.7	11.0

1/16-in. Flux Cored Open-Arc Electrodes

Expmt. no.	904	984	985	986	996	997	998	999
C	0.023	0.023	0.023	0.025	0.023	0.022	0.022	0.022
Mn	1.60	1.80	1.75	1.90	1.60	1.59	1.49	1.38
P	0.031	0.029	0.027	0.027	0.028	0.027	0.027	0.028
S	0.007	0.006	0.005	0.006	0.005	0.005	0.006	0.005
Si	0.42	0.61	0.62	0.62	0.44	0.52	0.38	0.39
Cr	22.07	21.92	22.29	21.85	21.93	22.14	22.31	21.93
Ni	8.70	8.55	8.55	8.55	8.35	8.45	8.50	8.40
Mo	3.88	3.26	3.50	3.40	3.40	3.42	3.48	3.32
Ti	0.23	0.23	0.33	0.54	0.13	0.13	0.05	0.05
N	0.126	0.150	0.126	0.137	0.154	0.170	0.165	0.170
EFN	60	50	87	117	46	53	38	34
Fe	62.9	63.4	62.8	62.9	63.9	63.5	63.6	64.3
EFN/NFN	1.407	1.416	1.404	1.407	1.426	1.418	1.419	1.433
NFN	43	35	62	83	32	37	27	24
UTS (ksi)	113.4	116.0	115.1	107.3	116.6	118.1	116.5	116.4
YS (ksi)	88.2	85.2	92.4	92.5	86.3	88.0	83.4	88.0
% Elongation	28	31	14	5	30.5	34	30	32
CVN@ −50°F (ft-lb)	35.6	33.7	25.9	16.3	38.2	32.7	50.0	49.9
mils	19.0	17.2	13.0	6.2	23.8	17.2	27.8	25.6

standard in the United States and has recently been adopted worldwide as ISO 8249-1985, can be extended to cover duplex stainless steel weld metals by the addition of counterweights to a Magne Gage and extrapolation of the calibration line (Ref. 5). This extended ferrite number (EFN) system was shown in Ref. 5 to provide good laboratory-to-laboratory reproducibility on duplex stainless steel weld metals.

Also in Ref. 5, it was shown, at least for cast metals, that the FN or EFN overestimates the volume percent ferrite by a factor that can be easily estimated from the iron content of the alloy. For cast alloys, a 1:1 agreement was found between a normalized ferrite number (NFN) and metallographically determined volume percent ferrite (which, on coarser cast alloy structures, has been established as having good lab-to-lab reproducibility, in contrast to the situation with weld metals). The correcting factor, which is divided into the EFN to obtain the NFN, increases with increasing iron content in the alloy. While it is presently impossible to establish the agreement between volume percent ferrite in weld metal and the NFN because there is no known reproducible way to establish the true volume percent ferrite in weld metal, it is believed by the author that the NFN is a reasonable approximation of the volume percent ferrite in weld metal.

In the present work, the major emphasis is on characterizing the ferrite content of the experimental weld metals by EFN because no approximations need be made in arriving at the EFN. NFN values are also reported as an indication of the volume percent ferrite, although it should be borne in mind that, especially for the Alloy 255 weld metals, the iron contents are lower than those explored in Ref. 5, and therefore, the correction factor estimated by the approximation given in Ref. 5 may be inadequate.

Experimental Program

The principle concern in this program was the mechanical properties of all-weld-metal in the as-welded condition. Two alloys were considered, Alloy 2205 and Alloy 255. Alloy 2205 was considered in more depth than the other alloy because it was the first alloy investigated in this program and there were no guidelines that would let one anticipate the extent of effects of ferrite content upon mechanical properties. When the pattern became clear, then a smaller number of compositions for Alloy 255 was investigated to see if the same general trends would be followed.

Experimental electrodes in the form of self-shielded flux cored wires were produced in either of two diameters, 1/16 in. and 3/32 in. (1.6 and 2.5 mm). With each electrode, an eight-layer pad for chemistry and ferrite determinations was deposited between copper blocks on a mild steel base plate, the same as would be used for covered stainless electrodes classified to AWS A5.4-80. After each of the first six layers was deposited (one pass per layer, approximately 3/4 in./19 mm wide), the pad was water quenched to below 300°F (149°C) without regard to the temperature at time of quench. For the seventh and eighth layers, since ferrite is transforming to austenite in these alloys as they cool, the deposit was allowed to air cool to black heat before quenching. Slag cover was removed after each pass.

After the pad had cooled to room temperature, the top surface of the last layer of weld metal was ground smooth on a 600 grit belt sander. (Earlier work had shown that coarser grit left a surface roughness that resulted in an artificially low reading when a Magne Gage was used for EFN determinations. The surface left by 600 grit gave virtually identical readings to those from a metallographically polished surface.) Five readings were then taken with a counterweighted Magne Gage along the deposit centerline, avoiding the first and last 2 in. (arc start and crater) of the deposit. The EFN for each reading was then calculated according to the method of Ref. 5, after which the average of the five readings was calculated and rounded to the nearest whole number for reporting.

Complete chemical analysis was then performed upon the metal of the last weld pass on each pad, again avoiding the arc start and crater. Chips were milled for carbon, sulfur, nitrogen, nickel, copper, phosphorus and chromium determinations, using wet or fusion analytical

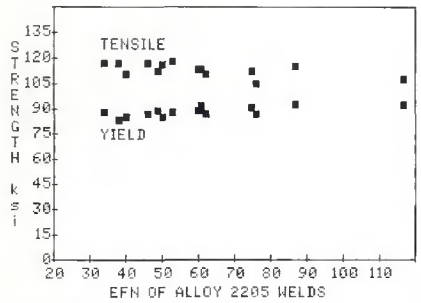

Fig. 1—Tensile and yield strength as functions of extended ferrite number of Alloy 2205 welds

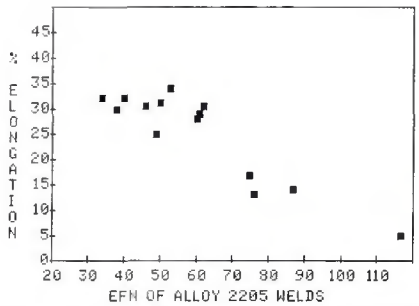

Fig. 2—Ductility as a function of extended ferrite number of Alloy 2205 welds

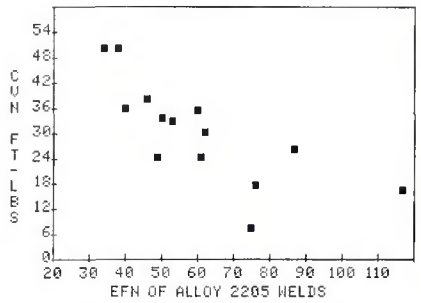

Fig. 3—Charpy V-notch energy absorbed at −50°F as a function of extended ferrite number of Alloy 2205 welds

techniques. X-ray spectroscopy was used for molybdenum, manganese, silicon and titanium determinations.

For mechanical property determinations, a groove weld in double-buttered ¾-in. (19-mm)-thick mild steel plate was prepared following the procedure which would be required for classification of the electrode according to AWS A5.22-80. After a single-pass root, all subsequent layers in the groove welds were deposited in two passes per layer. For both the pad and the groove welds, 3/32-in. (2.5-mm) electrodes were welded DC electrode positive, 275–300 A, 28 V, 1¼-in. (31.7-mm) electrode extension. The 1/16-in. (1.6-mm) electrodes were welded under the same conditions, except 210–230 A and ¾-in. (19-mm) electrode extension. An interpass temperature of 300°F (149°C) was maintained during preparation of each groove weld. The groove weld was allowed to air cool to room temperature upon completion of welding.

From each groove weld, a ½-in. (12.7-mm)-diameter longitudinal tensile specimen along the centerline and near the top surface of the weld was machined. As a precaution against possible diffusible hydrogen damage to tensile elongation, the tensile specimen was aged 48 hours at 212°F (100°C) before tensile testing. In addition to the tensile specimen, five full-size Charpy V-notch specimens, transverse to the weld with the notch on the groove centerline and perpendicular to the weld surface, were machined. These were all broken at −50°F (−46°C) and the results were averaged for reporting.

Alloy 2205 Experiments

A total of 14 experimental compositions approximating Alloy 2205 were produced as self-shielded flux cored electrodes. The main composition variable was initially nickel. Nickel content was varied from a near match to the base metal (about 5%) up to about 8.5%, to vary the ferrite content of the weld deposit. Titanium above a certain residual amount was also investigated. Certain compositions were repeated (approximately), using variations of the fluorspar slag system to observe if the slag system variations had any effect upon mechanical properties.

Table 2 lists the Alloy 2205 experimental compositions and test results. It is evident that the nickel content matching the base metal results in a high ferrite content, even when chromium is rather low and nitrogen is rather high, Weld Number 817. Titanium above residual levels has a very potent effect upon ferrite, as can be seen in Table 2 by comparing Welds 984, 985 and 986. The titanium effect is probably due to the formation of nitrides, which removes the potent austenitizing effect of nitrogen in solution.

It is interesting to note that the tensile and yield strengths are scarcely affected by EFN variation from as low as 34 to as high as 117. This is depicted graphically in Fig. 1. However, the ductility (percent elongation) and Charpy V-notch results at −50°F are markedly affected by the EFN of the deposit. Figure 2 demonstrates this effect for ductility, while Fig. 3 demonstrates this effect for Charpy V-notch results. Figure 2 indicates that ductility holds steady at about 30% elongation from low EFN up to at least 60 EFN, then undergoes a rather sharp transition to about 15% elongation at about 75 EFN, and declines further at higher EFN. In terms of NFN, the ductility transition occurs between 43 and 49 NFN. Figure 3 shows a more or less steady decline in Charpy V-notch energy at −50°F with increasing EFN, although there is considerable scatter.

Figure 4 compares the microstructure of a ductile weld of 46 EFN with that of a relatively brittle weld of 87 EFN. It can be seen that the ductile weld is characterized by austenite around the as-cast prior delta ferrite grain boundaries and considerable Widmanstätten austenite within the prior delta ferrite grains. On the other hand, the relatively brittle weld is characterized by columnar delta ferrite grains with austenite around the grain boundaries and not very much austenite within the delta ferrite grains. The fractured tensile specimens of the relatively brittle welds all showed areas of coarse crystalline facets resulting from fracture within the columnar ferrite (see Fig. 5), while the ductile weld tensile specimens all showed fine grained ductile fracture surfaces.

Alloy 255 Experiments

Because of a concern that Alloy 255 weld metals might require higher molybdenum than the corresponding base metal for adequate corrosion resistance in certain media, two molybdenum levels of about 3.5% and just over 4% were investigated. Nickel and titanium were varied

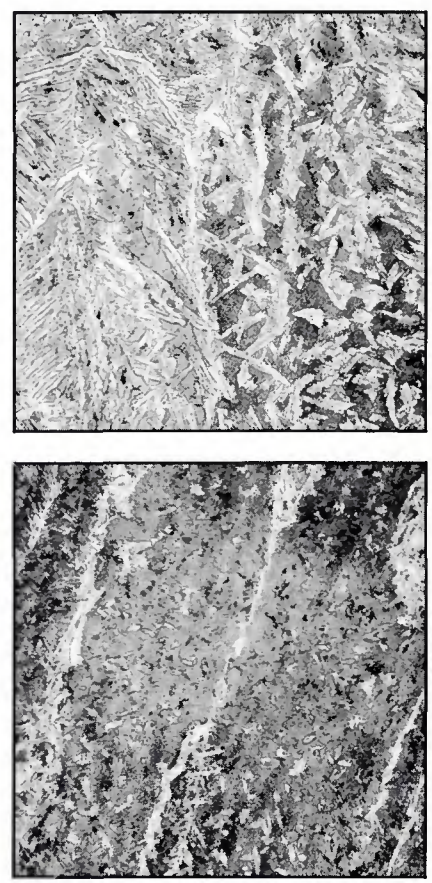

Fig. 4—Microstructures of Alloy 2205 welds 200X, Kallings reagent. Top—Weld 996, 46 EFN; Bottom—Weld 985, 87 EFN. Ferrite appears dark in these microstructures

Table 3—Alloy 255 (25Cr-5Ni-3Mo-2Cu) Experimental Welds

1/16-in. Flux Cored Open-Arc Electrodes						
Expmt. no.	004	012	013	014	053	054
C	0.044	0.050	0.047	0.048	0.022	0.026
Mn	1.33	1.12	1.14	0.95	0.90	0.91
P	0.027	0.025	0.024	0.022	0.025	0.030
S	0.007	0.005	0.006	0.014	0.014	0.013
Si	0.47	0.56	0.56	0.42	0.21	0.17
Cr	24.41	24.71	24.24	24.62	25.28	25.22
Ni	10.00	9.10	9.45	10.80	9.20	9.35
Mo	3.28	3.32	4.00	4.08	4.27	4.27
Cu	2.03	1.85	1.87	2.10	2.04	1.97
Ti	0.21	0.11	0.11	0.11	0.13	0.01
N	0.112	0.163	0.169	0.166	0.115	0.112
EFN	56	47	49	36	73	88
Fe	58.1	59.0	58.4	56.7	57.8	57.9
EFN/NFN	1.314	1.332	1.320	1.287	1.309	1.311
NFN	43	35	37	28	56	67
UTS (ksi)	124.8	126.8	126.3	123.8	*	*
YS (ksi)	93.6	95.4	99.6	90.5	*	*
% Elongation	27	24	12	14	*	*
CVN@ −50°F (ft-lb)	27.0	28.9	20.8	15.3	8.9	18.0
mils	13.8	13.4	9.6	6.0	1.2	2.8

1/16-in. Flux Cored Open-Arc Electrodes				
Expmt. no.	055	056	057	112
C	0.022	0.024	0.021	0.014
Mn	1.00	0.97	0.97	1.06
P	0.025	0.023	0.021	0.026
S	0.014	0.007	0.008	0.005
Si	0.25	0.32	0.31	0.36
Cr	25.25	24.79	24.58	24.51
Ni	9.30	10.25	10.95	10.17
Mo	3.46	3.64	3.56	3.18
Cu	2.02	2.02	2.11	2.14
Ti	0.13	0.02	0.02	0.02
N	0.110	0.135	0.118	0.084
EFN	75	44	35	53
Fe	58.4	57.8	57.3	58.4
EFN/NFN	1.321	1.309	1.300	1.321
NFN	57	34	27	40
UTS (ksi)	*	122.1	121.6	121.8
YS (ksi)	*	91.1	90.9	89.6
% Elongation	*	30	28	25
CVN@ −50°F (ft-lb)	17.6	27.3	26.2	26.3
mils	5.4	13.2	13.4	12.3

*Groove weld developed transverse cracks about two hours after welding was completed. Tensile properties could not be measured, but CVN specimens could be taken.

over a smaller range in this series because their effects were already understood from the Alloy 2205 series. The compositions and test results are shown in Table 3.

That molybdenum does not have an especially potent effect on promoting ferrite can be seen by comparing Welds 012 and 013. From the four welds of about 4% molybdenum, it can, however, be seen that molybdenum of this level is very detrimental to ductility, even at rather low ferrite levels, as in Welds 013 and 014, as compared to Welds 012 and 056. The three highest ferrite welds, 053, 054 and 055, have no tensile data in Table 3 because all three weldments developed transverse cracks approximately 2 h after each weldment was completed. Such delayed cracking is likely due to diffusible hydrogen, which can move readily through ferrite.

The five welds of about 3.5% molybdenum in Table 3 all exhibited high ductility, and Charpy V-notch energies above 20 ft-lb at −50°F. These are all of less than 60 EFN, so they behave exactly as did the welds of Alloy 2205. The 3.5% molybdenum weld with high ferrite (Weld 055) had poor Charpy V-notch values at −50°F and no ductility, which is consistent with the behavior of the Alloy 2205 welds of similar ferrite content.

Figure 6 compares microstructures of Alloy 255 welds of about 3.5% molybdenum with ferrite below and above 60 EFN. As with the Alloy 2205 welds, the lower ferrite microstructure shows austenite around the prior delta ferrite grain boundaries and extensive Widmanstätten

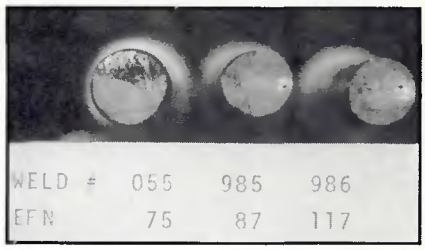

Fig. 5—Fractured tensile specimens of Alloy 255 weld (055) and Alloy 2205 welds (985 and 986), all having high ferrite. The Alloy 255 weld was cracked before tension testing. The Alloy 2205 welds developed coarse crystalline facets on their fracture surfaces during testing

austenite within the ferrite grains. The higher ferrite weld microstructure is marked by columnar ferrite with austenite on the grain boundaries, but relatively little austenite within the columnar ferrite grains.

Figure 7 presents a high magnification microstructure of a lower ferrite weld of more than 4% molybdenum. The etch, 10% chromic acid, applied electrolytically, is supposed to preferentially attack sigma phase. This view indicates something within some, but not all, of the ferrite regions which is preferentially attacked. This attack is not apparent in the lower molybdenum weld deposits. It was initially considered that the constituent attacked was sigma or chi phase, either of which could account for the brittleness of the weld deposits containing it. It was noted that this constituent tended to be present mainly in regions where the ferrite was coarser than average.

This constituent was examined in more detail with the aid of a scanning electron microscope (SEM) with x-ray dispersive analytical capability. Figure 8 shows a concentration of particles of this constituent in a coarse ferrite region and the absence of the particles in the nearby finer ferrite regions. One notes in Fig. 8 that some of the particles appear acicular, while others appear equiaxed. The acicular particles appear somewhat larger than the equiaxed particles. Since two shapes might indicate two different phases, point counts were attempted on each shape of particle. Table 4 lists some typical results.

Comparing the composition of the ferrite matrix to that of the acicular particles leads to the conclusion that the acicular particles are austenite. This "secondary austenite" is more than an order of magnitude finer than the primary austenite between ferrite grains.

It was difficult to maintain the electron beam on the equiaxed particles, and the point analyses on these particles all show molybdenum levels like that of the ferrite, but lower chromium and higher nickel than that of the ferrite. So they are clearly

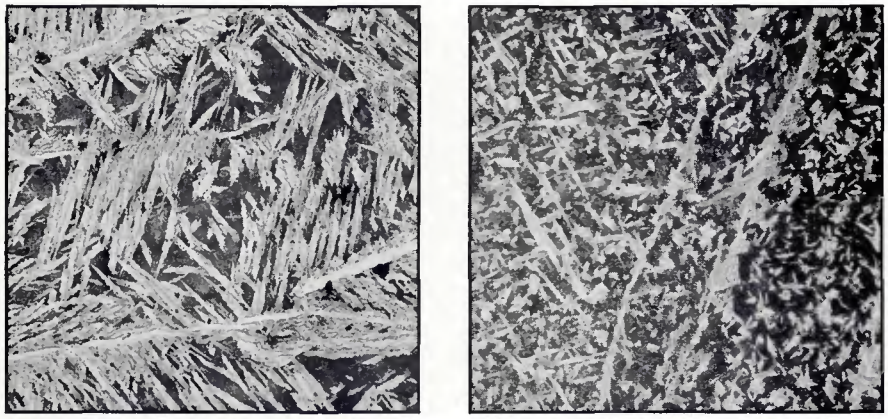

Fig. 6—Microstructures of Alloy 255 welds 200X, Kallings reagent. Left—Weld 056, 44 EFN; Right—Weld 055, 75 EFN. Ferrite appears dark in these microstructures

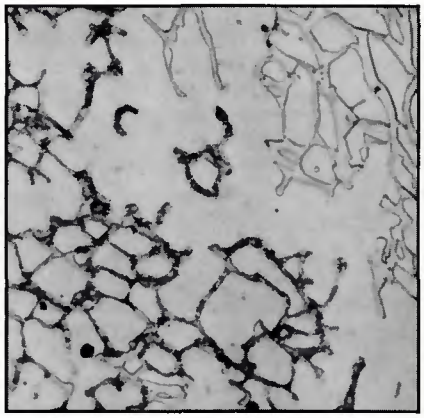

Fig. 7—Microstructure of Alloy 255 weld (014) 1330X, 10% chromic acid electrolytic etch. Some ferrite is clear, while other ferrite contains a second phase

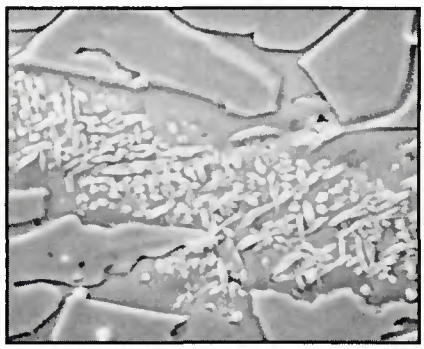

Fig. 8—Microstructure of Alloy 255 weld (014) 2800X, 10% chromic acid electrolytic etch, SEM image at 18 kv. Acicular and equiaxed particles within ferrite are visible

not sigma phase, but also appear to be secondary austenite. It is believed by the author that these particles are also acicular secondary austenite, but they obtain an equiaxed appearance by being sectioned perpendicular to their long axis.

Discussion of Results

The results of this study agree, in a qualitative sense at least, with the findings of Blumfield, Clark and Guha for Alloy 255, and with those of Bryhan and Poznansky for Alloy 2205. That is, for both alloys, considerably more nickel is necessary in the as-welded metal than in the heat-treated and/or hot-worked base metal to obtain reasonable weld metal ductility and toughness. A clearer understanding of the need for this higher nickel is apparent from the microstructural evidence of Figs. 4 and 6.

At nickel levels similar to those of the base metals, the as-cast structure of the weld deposit consists of coarse columnar ferrite grains with austenite nearly continuous along the ferrite grain boundaries, but there is not much austenite within the individual columnar ferrite grains. Then the effective grain size for crack propagation in this microstructure is the coarse columnar ferrite grain size. Rather large continuous crack paths are available in this ferrite. The large crystalline facets on the broken tensile specimens of Fig. 5 are further evidence of this continuous crack path.

On the other hand, when the nickel level is sufficiently high in an otherwise matching filler metal, then sufficient Widmanstätten austenite forms within the original columnar ferrite grains to break up the continuous crack paths within the ferrite. The austenite is appreciably tougher than the ferrite and serves as a crack stopper. It also reduces the effective grain size of the ferrite to that of the spacing between the Widmanstätten austenite grains. The net result is a much more ductile and tough material.

The apparent breaking up of the continuous columnar ferrite grains by Widmanstätten austenite probably accounts for the rather sharp transition in ductility observed as a function of ferrite content. This sharp transition in ductility has not been previously observed or reported as far as the author is aware.

The application of the extended ferrite number concept to evaluation of duplex stainless weld metals offers a nondestructive method of filler metal specification and quality assurance. While it may be possible to exceed 60 EFN slightly and still meet a 20% elongation requirement or a 20 ft-lb Charpy V-notch requirement at −50°F (−46°C), an upper limit of 60 EFN would offer assurance that good ductility and toughness will be obtained. The present work clearly demonstrates that the high yield strength of duplex stainless steels is preserved in the weld metal well below 60 EFN.

A low heat input weld might also have a different (probably higher) critical EFN at which the ductility transition takes place because its columnar ferrite grain size would be finer than in this study. The author's laboratory has observed good ductility in Alloy 255 shielded metal arc deposits of 70 EFN or slightly higher.

The cause of poor ductility in the Alloy 255 welds of slightly over 4% molybdenum is not understood. It is difficult to conceive that the formation of the observed secondary austenite alone is responsible for this. No direct evidence of sigma or chi phases was detected using the SEM. It is possible that the observed secondary austenite is but one of two decomposition products of ferrite, with the other decomposition product too small to be detected with the SEM (delta ferrite → austenite + sigma or chi). The formation of the secondary austenite within ferrite areas has to be accompanied by a local enrichment of nickel and a depletion of chromium and molybdenum where the austenite forms. Then there ought to be corresponding areas where

Table 4—SEM Point Analyses on Alloy 255, Weld 014, Second-Phase Particles within Delta Ferrite

Structure	Ferrite Matrix	Acicular Particles			Equiaxed Particles	
Point No.	1	2	3	4	5	6
Si	0.47	0.42	0.49	0.81	0.84	0.71
Cr	28.75	24.43	25.53	22.08	25.99	24.23
Mn	1.05	1.04	1.09	1.37	0.55	0.36
Fe	55.74	57.09	56.26	56.29	56.14	56.20
Ni	6.32	10.93	9.74	12.17	8.12	10.37
Cu	1.02	2.05	1.77	2.43	1.28	1.69
Mo	6.64	4.02	5.11	4.86	7.07	6.45

there is a local depletion of nickel and an enrichment of chromium and molybdenum, with such areas likely to transform to sigma or chi. But these have not been possible to detect within the limitations of the present work. This is only a hypothesis, of course.

The observation of delayed cracking in some of the Alloy 255 weldments is noteworthy. The cracked welds were all of 75 EFN or higher, and all such welds in this study cracked. Such welds are higher strength than the Alloy 2205 welds, which would make them more susceptible to hydrogen damage. At the same time, the microstructural observation of austenite along the columnar ferrite grain boundaries, but little austenite within the ferrite grains, makes it clear that there is considerable latitude for hydrogen to move within a given columnar ferrite grain. It is well known that the combination of high strength material, high residual stress, and diffusible hydrogen can produce such delayed cracking. Because the columnar ferrite grains are surrounded by austenite on their grain boundaries, it is difficult to see how this hydrogen could be effectively removed. A cursory attempt to measure this hydrogen in an Alloy 255 deposit, using the method of AWS A4.3-86, recovered no diffusible hydrogen. It is hypothesized that this is due not to the absence of diffusible hydrogen, but to austenite around the ferrite grain boundaries preventing hydrogen from escaping from the ferrite grains.

Conclusions

Based upon the results described herein, the following conclusions can be drawn:

1. The extended ferrite number (EFN) is a useful tool for characterizing and specifying duplex stainless steel weld filler metals.

2. Ferrite content below 60 EFN in nearly matching weld deposits for Alloys 2205 and 255 provides sufficient ductility and toughness that a side bend test can be passed and that Charpy V-notch energy of better than 20 ft-lb (14.7 J) at −50°F (−46°C) can be obtained.

3. Ferrite content above 30 EFN in the as-welded condition in nearly matching weld deposits for Alloys 2205 and 255 provides yield strength and tensile strength in the weld metal similar to those of the base metal.

4. Flux cored open-arc electrodes of about 8.5% nickel, which otherwise match Alloy 2205, provide appropriate ferrite for excellent mechanical properties in the as-welded condition in this alloy.

5. Flux cored open-arc electrodes of about 10% nickel, which otherwise match Alloy 255, provide appropriate ferrite for excellent mechanical properties in the as-welded condition in this alloy.

6. Molybdenum enrichment to 4% as an approach to enhancing the corrosion resistance of Alloy 255 weld metal raises the distinct possibility of embrittlement, even at low ferrite contents.

7. Alloy 255 welds can be damaged by diffusible hydrogen, at least when their ferrite content is high enough to result in a microstructure that retains the original columnar delta ferrite in a continuous form. This could be of concern in matching composition welds intended for subsequent heat treatment (for example, casting repairs) or in a highly diluted root pass.

Acknowledgments

The author is grateful to Teledyne McKay for providing the environment and resources to pursue this work, and to Stanley J. Merrick for considerable assistance in the metallography portion of the work.

References

1. Blumfield, D., Clark, G. A., and Guha, P. 1981. Welding duplex austenitic-ferritic stainless steel. *Metal Construction* (5):269-273.

2. Bryhan, A. J., and Poznansky, A. 1984. Evaluation of the weldability of ES2205. Report CP-280, AMAX Metals Group, Ann Arbor, Mich.

3. AWS A4.2-86. 1986. *Standard Procedures for Calibrating Magnetic Instruments to Measure the Delta Ferrite Content of Austenitic Stainless Steel Weld Metal.* American Welding Society, Miami, Fla.

4. Pleva, J., and Nordin, S. 1983. Properties of different MMA-welds on modified Type 329 ferritic-austenitic stainless steel. Paper #8201-030, pp. 603-629, *Duplex Stainless Steels,* American Society for Metals, Metals Park, Ohio.

5. Kotecki, D. J. 1982. Extension of the WRC ferrite number system. *Welding Journal* 61(11):352-s to 361-s.

6. ASTM A240-85. *Standard Specification for Heat-Resisting Chromium and Chromium-Nickel Stainless Steel Plate, Sheet, and Strip for Pressure Vessels.* American Society for Testing Materials, Philadelphia, Pa.

KEY WORDS
Weld Ferrite Content
Ferrite in Duplex SS
Extended Ferrite No.
22Cr-5Ni-3Mo Alloy
25Cr-5Ni-3Mo-2Cu-58Fe
Flux Cored Wire Wldg
Ni for Ductility
Ni for Toughness
Ductility Transition
Toughness at −50°F